Mechanical Unfolding of Segment-Swapped Protein G Dimer: Results from Replica Exchange Molecular Dynamics Simulations

Pai-Chi Li, Lei Huang, and Dmitrii E. Makarov*

Department of Chemistry and Biochemistry and Institute for Theoretical Chemistry, University of Texas at Austin, Austin, Texas 78712

Received: November 7, 2005; In Final Form: May 14, 2006

The protein G dimer (pdb code 1Q10) is a mutated dimeric form of the immunoglobulin-binding domain B1 of streptococcal protein G, in which the two monomeric units have swapped elements of their secondary structure. We have used replica exchange molecular dynamics simulations to study how this dimer responds to a mechanical force that pulls the N-terminus of one unit and the C-terminus of the other apart. We have further compared the mechanical response of the dimer to that of the protein G monomer. When the pulling force is low enough, the mechanical unfolding can be viewed as a thermally activated barrier crossing process. For each protein, we have computed the corresponding free energy barrier and its dependence on the pulling force. While the dimer is found to be less resistant to mechanical unfolding than its monomeric counterpart, the two proteins exhibit essentially the same mechanical unfolding mechanism involving separation of the terminal parallel strands. On the basis of our results, we speculate that the mechanical properties of natural adhesives, composites, fibers, and other materials may be optimized not only at a single molecule level but also at the mesoscopic level through the interactions among individual chains.

1. Introduction

Unique mechanical properties of natural fibers, adhesives, and composites can often be linked to the mechanical response of individual proteins they are composed of.[1] The mechanical properties of a number of individual "load-bearing" protein domains, as well as other domains that have no apparent mechanical function, have been well characterized both experimentally (via single-molecule pulling experiments) and computationally (via molecular dynamics studies), see refs 2−4 and the references therein. At the same time, there is a gap between our understanding of the mechanical response of proteins at the single-molecule level and that of the bulk materials they form. Since the latter usually involve complex assemblies of proteins, it is not clear to which extent their overall mechanical properties are controlled by the mechanical stability of individual domains as opposed to interchain interactions and the overall architecture of the material. Here, we study the mechanical response of the simplest possible protein complex, a protein dimer, when the C-terminus of one of its subunits and the N-terminus of the other are pulled apart. Being a dimer, in which segments of secondary structure are interchanged between the two monomers, its mechanical properties cannot be simply derived from those of its monomeric units.

We are particularly interested in finding out whether the unique mechanical stability achieved by Nature in some of its load-bearing proteins[5−11] can be retained when such proteins are assembled noncovalently to form complexes. There are very limited experimental data regarding the mechanical properties of protein complexes in general and dimers in particular[12,13] so we have to rely on simulations. Fortunately, previous studies have shown that simulations can lead to quantitative predictions regarding the mechanical strength of proteins.[9,14−19] Related simulation studies of forced dissociation of adhesion protein complexes have recently been reported by others,[20,21] providing a different example of the mechanical response of a protein complex.

The present study may have implications for several other topics of current interest. Segment-swapped dimers are often viewed as models of protein aggregation.[22] While it is now understood[6,10,17,18,23−27] that mechanical unfolding experiments do not necessarily probe proteins' thermodynamic stability and their folding and/or chemical/thermal denaturation pathways, they may still offer insight into the stability of protein aggregates. Furthermore, mechanical response of protein aggregates is of interest since it is believed that the cellular machinery responsible for protein degradation unfolds them by pulling them mechanically through narrow constrictions,[28−30] and since there is evidence that this machinery attempts to unfold protein aggregates.[28]

Many naturally occurring protein complexes, or multimers, are assemblies of two to thousands of protein domains. They perform a variety of tasks including mechanical functions (e.g., in the case of collagen or cadherins). In segment-swapped dimers,[31] each domain exchanges part of its secondary structure with neighboring domains.

The specific case of a segment-swapped dimer studied here is the dimeric mutant Q10 of the B1 domain of streptococcal protein G,[32,33] which has been engineered[32,33] by introducing mutations in the core amino acids of the domain B1 of streptococcal protein G (GB1).[34] The structure of this dimer (Figure 1) involves terminal parallel strands formed by exchanging the terminal β-strands of the two monomeric subunits. If a stretching force is applied between the N-terminus of chain A and the C-terminus of chain B as shown in Figure 1 (right), the two parallel strands become loaded in a manner similar to that found in a pulling experiment where a single GB1 domain is stretched between its C- and N-termini (as shown in Figure 1,

* To whom correspondence should be addressed. E-mail: makarov@mail.cm.utexas.edu.

10.1021/jp056422i CCC: $33.50
Published on Web 07/06/2006

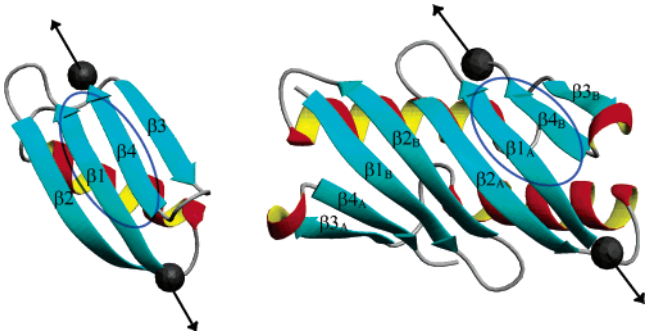

Figure 1. Left: The NMR structure of the immunoglobulin-binding domain B1 of streptococcal protein G, 1GB1. Right: the structure of the segment-swapped dimeric mutant of the B1 domain of streptococcal protein G (1Q10). In our simulations, the stretching force is applied between the α-carbons of the terminal residues shown as dark spheres. Labeled elements of secondary structure are the strands $\beta 1$ (residues 2−8), $\beta 2$ (residues 13−19), $\beta 3$ (residues 42−46), and $\beta 4$ (residues 51−55) for the monomer and the strands $\beta 1$ (residues 2−8), $\beta 2$ (residues 13−19), $\beta 3$ (residues 43−46), and $\beta 4$ (residues 51−54) for each monomer of the dimer; the subscript labels the chains A/B. The location of the terminal parallel strands in each protein is circled. The plots were generated by the MOLMOL software.[63]

left). It has been recently understood that this type of arrangement of parallel strands is the key structural feature responsible for the high mechanical stability of the I27 domain of the muscle protein titin.[15,17,24] Furthermore, it was predicted theoretically[7−9] and established experimentally[6,10,11,18] that other domains (e.g., protein L and ubiquitin), which have no apparent mechanical function but feature the same terminal strand arrangement may exhibit high mechanical stability comparable to that of I27. Therefore if the high mechanical resistance with respect to stretching typical of some individual domains can be retained by protein complexes, the above dimer structure appears to be a good candidate. In what follows, we present a comparative study of the mechanical stability of the protein G dimer stretched between the C-terminus of one subunit and the N-terminus of the other (Figure 1) with that of the monomeric protein G.

The rest of this paper is organized as follows: in section 2, we describe the details of the methods used. Our results are presented in section 3, and section 4 concludes.

2. Methods

Recent studies[9,17] showed that mechanical unfolding of proteins in many cases can be understood, quantitatively, by using a simple one-dimensional picture, where it is viewed as Langevin dynamics governed by the potential of mean force $G(R)$ that is a function of the "mechanical" reaction coordinate R.[16] The latter is usually chosen to be equal to the protein extension, i.e., the distance between the residues (or, more precisely, between their α-carbons) between which the pulling force is applied. The potential of mean force $G(R)$ can be computed using the standard umbrella sampling method,[35,36] where a penalty term constraining the extension to a neighborhood of R is added to the system energy; the shape of $G(R)$ is then obtained from a series of equilibrium molecular dynamics (MD) simulations performed with different constraints. By combining the data from such simulations via the weighted histogram method,[36] one can recover the global shape of $G(R)$. The technical details of this procedure as applied to protein stretching are described in ref 9.

Whenever one attempts to calculate an equilibrium property of a protein such as $G(R)$, there is a concern as to whether the configuration space of the protein is sampled ergodically within the time-scale constraints of the simulation. Although it is impossible to guarantee complete sampling in any simulation, dependence of the simulation result on the length of the simulation would be a clear indication of trouble. In our previous studies of the mechanical stretching of small domains, the results appeared converged with respect to the length of each equilibrium MD simulation.[9,17,18] However for the protein G dimer we could not obtain converged results with the simulation times feasible given the computer resources available to us. This urged us to resort to the replica exchange method (REM), which provides better sampling. The method is reviewed in ref 36, and its specific implementation in MD simulations has been developed in ref 39. REM/MD involves running MD trajectories for a set of n replicas of the system, each at different temperature: T_i ($i = 1, 2, ..., n$), such as $T_1 < T_2 < ... < T_n$.

The algorithm further includes Monte Carlo trial moves that attempt to "swap" neighboring replicas. A trial move attempting to swap the configurations $\mathbf{r}_i$ and $\mathbf{r}_{i+1}$ of the replicas running at the temperatures T_i and T_{i+1} is accepted with a probability equal to min $\{1, \exp[-(\beta_{i+1} - \beta_i)(U(\mathbf{r}_{i+1}) - U(\mathbf{r}_i))]\}$, where U is the potential energy of the system and $\beta_i = 1/(k_B T_i)$, where k_B is Boltzmann's constant. The velocities of each atom are rescaled after the trial move such that the new velocities satisfy the equipartition theorem.[37] Such trial moves satisfy detailed balance and help the low-temperature replicas that are trapped near local minima on the system's potential energy landscape overcome barriers separating those from other regions of the configuration space.

By use of REM combined with umbrella sampling, we have reconstructed the potential of mean force $G(R)$ in the cases of the stretching of protein G (pdb code 1GB1) and the protein G dimer (pdb code 1Q10). The reaction coordinate R is defined as the distance between the α-carbons of the two terminal residues (Met1 and Glu56) in the case of the protein G monomer and the distance between the α-carbon of the Met1 in the chain A and the α-carbon of the Glu56 in the chain B in the case of the dimer. A harmonic penalty term $\gamma(R - R_0)^2/2$ was added to the energy to constrain the protein extension near a specified value R_0 in umbrella sampling simulations,[9,17] with the spring constant $\gamma = 1.38$ N/m. The values of R_0 used were $R_0 = 26.7$, 27.7, 28.7, 29.7, 30.7, 31.7, and 32.7 Å for protein G, and $R_0 = 25.8$, 26.8, 27.8, 28.8, 29.8, 30.8, and 31.8 Å for the dimer. For each R_0, we have used $n = 10$ replicas run at the temperatures (273, 285, 298, 312, 327, 343, 361, 379, 399, and 422 K). The results reported below are for $T = 298$ K.

Simulations were performed with Tinker software (http://dasher.wustl.edu/tinker/) using the GB/SA continuum solvation model,[38] and the AMBER99 force field.[39] Both the monomeric and the dimeric protein G remain nativelike in the course of a 0.5-ns unconstrained simulation at 298 K, using this force field/solvation model. The Rattle algorithm[40] was used to fix all the bond lengths between hydrogen atoms and heavy atoms. The MD time step was 2.0 fs, and a replica-swapping move was applied every 1.0 ps of the simulation. Protein configurations were saved every 0.5 ps. The total simulation time for each replica was 0.5 ns for each constraint and each temperature.

3. Results

In Figure 2, we show the free energy profile $G(R)$ as a function of the protein extension for the protein G monomer (GB1) and the dimer (Q10). The protein extension, $\Delta R = R - \langle R_{fold} \rangle$, is defined as the distance R between the α-carbons of the terminal residues that are being pulled apart relative to the average extension $\langle R \rangle \equiv \langle R_{fold} \rangle$ measured in the equilibrium

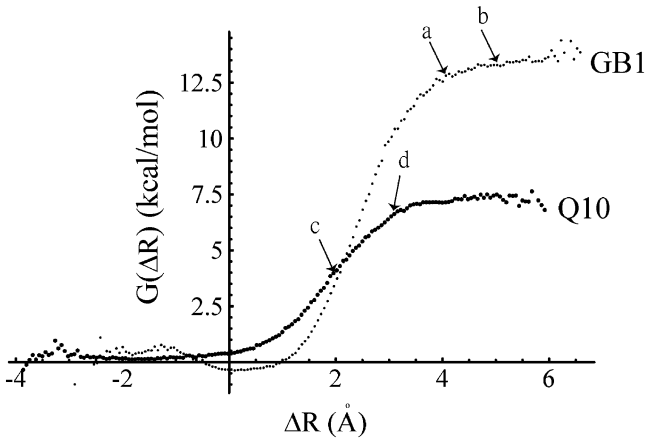

Figure 2. The free energy of GB1 and Q10 as a function of the extension. The two arrows near each curve roughly delineate the region where the separation of the terminal parallel strands takes place. Domain configurations corresponding to these values of extension are further analyzed in Figures 5−6. The positions ΔR of the arrows are: (a) 4.1 and (b) 5.1 Å for GB1 and (c) 2.1 and (d) 3.1 Å for Q10.

MD simulation in the absence of force. $<R_{fold}>$ is equal to 27.61 and 27.73 Å for GB1 and Q10, respectively. The free energy of protein reconstructed from the REM/MD with the smallest constrain R_0 is taken as the reference. The negative value of extension shown in the Figure 2 is simply due to the fact that $<R_{fold}>$ is larger than the smallest constrain distances R_0 (i.e., 26.7 and 25.8 Å for GB1 and Q10), which are measured in the crystal structures of GB1 and Q10. The shapes of the two curves are very similar. They are also similar to the free energy profiles found in our previous studies of ubiquitin-like domains and I27.[9] The free energy $G(R)$ rises monotonically until it reaches a plateau value G_{pl}. This value is $G_{pl} \approx 14$ kcal/mol for the monomer and ≈7 kcal/mol for the dimer. The value of $G_{pl} \approx 14$ kcal/mol is similar to the value $G_{pl} \approx 17$ kcal/mol found in our previous study of the protein G IgG-binding domain III, which has similar structure.[9]

When the stretching force f applied to the protein is not too high, the unfolding dynamics can be viewed as barrier crossing.[41−44] Specifically, the potential of mean force experienced by the protein is equal to

$$G_f(R) = G(R) - fR$$

This force-dependent free energy profile is shown in Figure 3 for both proteins at different values of the stretching force. Application of a force turns the global minimum corresponding to the native fold into a metastable state separated from the extended states with large R by a barrier. The height of this barrier determines the rate constant of mechanical unfolding, which can be estimated by using transition-state theory

$$k_u(f) = \nu \exp(-\Delta G_u/k_B T).$$

Here

$$\Delta G_u(f) = G(R^{\neq}) - G(R_N)$$

is the free energy barrier, i.e., the difference between $G(R)$ at the minimum R_N corresponding to the native metastable state and the maximum $R^{\ddagger}$ corresponding to the transition state. The transition state extension $\Delta R^{\ddagger} = R^{\ddagger} - R_N$ determines how fast $k_u(f)$ changes as a function of the stretching force. It consequently impacts the pulling rate dependence of the average unfolding force measured in atomic force microscopy (AFM) pulling experiments.[43,44]

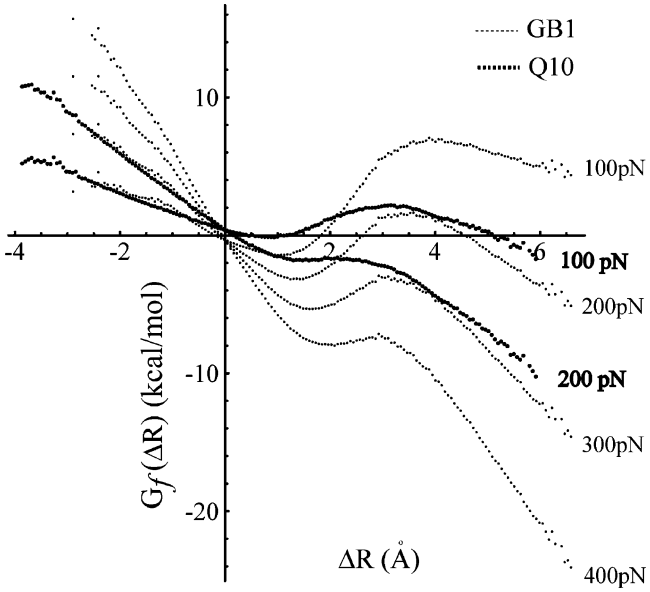

Figure 3. The free energy $G_f(\Delta R) = G(\Delta R) - f\Delta R$ for different values of the stretching force f.

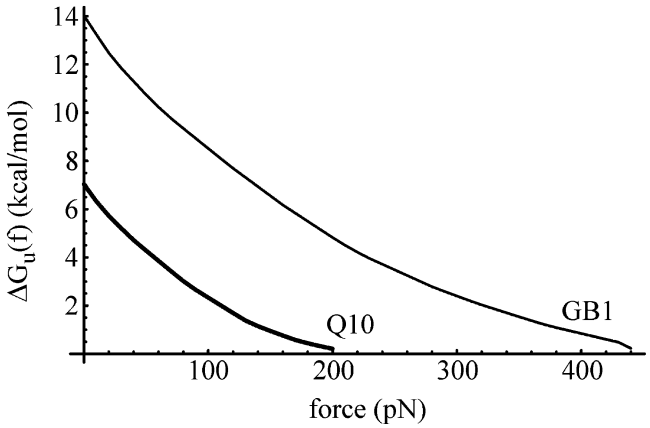

Figure 4. The unfolding free energy barrier $\Delta G_u(f)$as a function of the applied force for GB1 and Q10. The barriers were calculated starting from $f = 0$ pN with an increment of 10 pN. The continuous lines were obtained by interpolation.

As seen from Figure 3, the values of $\Delta R^{\ddagger}$ are similar for both the dimer and the monomer. For example, for $f = 100$ pN, $\Delta R^{\ddagger} \approx 3$ Å in each case. As a result, the force dependence of the barrier $\Delta G_u(f)$is similar in the two cases, as shown in Figure 4. At a sufficiently high force, the unfolding free energy barrier disappears altogether, rendering the native conformation of the protein mechanically unstable. This critical force required to destabilize the native state of the protein mechanically is on the order of 200 pN for the dimer and ∼400 pN for the monomer.

To understand the unfolding mechanism better, we next consider the protein configurations at different stages of the unfolding process. A convenient way to represent an ensemble of configurations sampled by a protein is its contact map. For a given configuration we define the contact map as the plot of residue pairs $\{i,j\}$ such that the distance between their respective α-carbon atoms is less than a given cutoff distance d. We use the value $d = 7.5$ Å here. To see how the protein structure depends on its extension, we have examined the equilibrium ensembles of protein structures obtained via the constrained

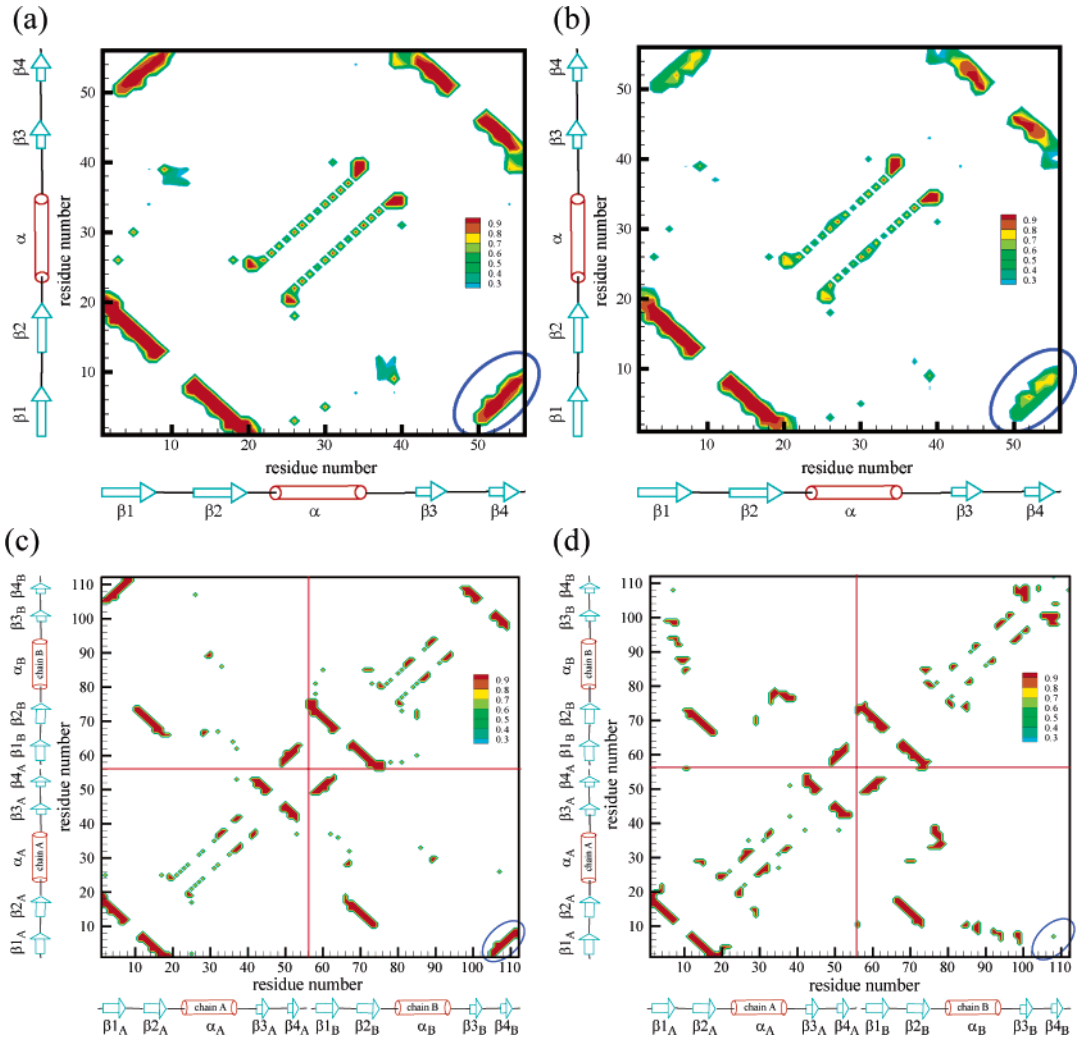

Figure 5. The contact maps of (a,b) GB1 and (c,d) Q10 obtained from equilibrium MD runs with the protein extension ΔR constrained near the values indicated as arrows in Figure 2. (a) $\Delta R_a \approx 4.1$ Å; (b) $\Delta R_b \approx 5.1$ Å; (c) $\Delta R_c \approx 2.1$ Å; (d) $\Delta R_d \approx 3.1$ Å. The terminal parallel strands shown in Figure 1 are indicated by the blue circles on each contact map. See text for further details.

equilibrium REM/MD runs as described in section 2. For a given constraint R_0, and for each contacting pair $\{i,j\}$, we then consider the probability of observing this contact in the equilibrium ensemble (i.e., the fraction of configurations for which their α-carbons are found within the distance d). In Figure 5, we color code the $\{i,j\}$ map according to these probabilities. This results in a contact map that describes an ensemble of structures rather than a single structure.

Parts a and b of Figure 5 display the contact maps for the monomeric protein G obtained for two different values of extension R_0, which are indicated by arrows in Figure 2. It is tempting to identify those as "pre-transition-state" and "post-transition-state" ensembles; however, as seen in Figure 3, the location of the transition state generally depends on the applied force so the transition-state extension is not well defined. Instead, we simply consider the changes in the protein structure as its extension is increased. Initially, the contact map remains virtually unchanged and similar to the native contact map (not shown). In particular, the contact map shown in Figure 5a is essentially the native contact map indicating that the protein native structure remains intact upon initial stretching. As the domain extension is increased further, as in Figure 5b, and the free energy $G(R)$ approaches its plateau value G_{pl}, the contacts formed by the terminal parallel strands (encircled in Figure 5) become partially destroyed. There is no considerable change in the rest of the contact map. An example of a structure belonging to the partially unfolded ensemble corresponding to Figure 5b is shown in Figure 6a. Note that the entire ensemble cannot be generally represented by this single structure.

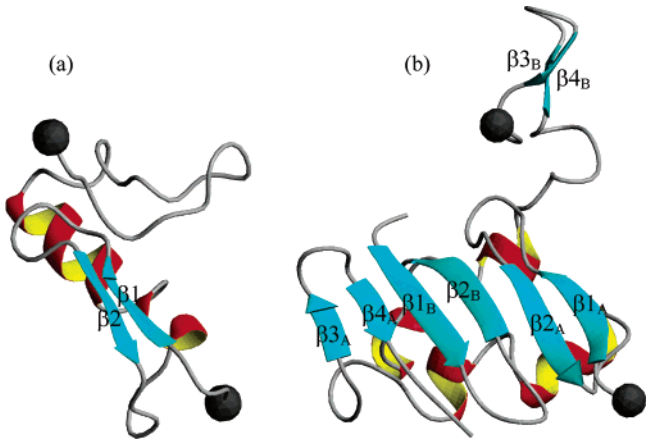

Figure 6. Two representative configurations of partially unfolded (a) GB1 and (b) Q10 taken from equilibrium ensembles corresponding to the situations depicted in parts b and d of Figure 5, respectively. The plots were generated by the MOLMOL software.[63]

Similar behavior is found in the case of the dimer (parts c and d of Figure 5). In this case the contact map consists of two diagonal blocks corresponding to the contacts among residues within the same monomeric unit and the off-diagonal blocks, which correspond to the contacts formed between different monomers. Notably, the parallel strands $\beta 1$ and $\beta 4$ of the protein G monomer become replaced by the parallel strands $\beta 1_{A(B)}$ and $\beta 4_{B(A)}$ formed across the monomers within the dimer. In addition to this parallel strand swapping, an additional pair of parallel strands ($\beta 2_A$ and $\beta 2_B$) is formed (see Figure 1). Similarly to the case of the protein G monomer, as the dimer is stretched initially, the native structure remains intact (case c in Figure 5). As R is further increased and $G(R)$ approaches its plateau value, the terminal parallel strands become disrupted as seen in Figures 5d and 6b.

The above unfolding mechanism proceeding via separation of the terminal parallel stands is similar to that observed in the simulations of I27,[14,15,17,45] ubiquitin,[9,18] and protein L.[11] This mechanism was predicted to maximize the mechanical strength of both proteins and toy models of cross-linked Gaussian polymers.[7,8]

We note that the shape of $G(R)$ for extensions much longer than those in Figures 2−3 is not readily accessible by MD simulations. The problem is that once the protein is unfolded or partially unfolded, the configuration space sampled by it becomes much larger while the time scale of its motion becomes slower. This necessitates much longer simulation times that are not feasible even when enhanced sampling methods such as REM are used. For these reasons, on the basis of our simulations alone, we cannot claim that the mechanical unfolding of each of the above proteins is an all-or-none process with a rate-limiting step being the separation of terminal strands. However this picture seems to be consistent with the experimental studies of titin[24,25,41,46,47], ubiquitin,[10,48,49] and protein L.[11] It is further consistent with Langevin dynamics simulations of a minimalist foldable off-lattice model of ubiquitin, which captures the folding time scale and allows one to map out the free energy landscape of this domain far from equilibrium.[23]

4. Discussion and Conclusions

All-atom studies of protein unfolding unavoidably have limitations. For example, the energy landscape and the native structure found from equilibrium REM simulations of the monomeric protein G show significant force field dependence.[50] The use of an implicit solvent model imposes another important limitation. When explicit solvent degrees of freedom are eliminated from the system, this results in additional effective solvent-induced forces.[51−54] These forces are not present in the standard continuum solvation model used here (see, e.g., refs 55 and 56). Solvent-induced forces are known to be important when considering protein−protein interactions and protein folding/unfolding.[57] In particular, correct description of hydrogen bonding interactions within a continuum model requires a very careful treatment of those effects.[57,58] Since the rupturing of the hydrogen bonds between the terminal strands arguably contributes a large part of the free energy barrier to unfolding,[14,15] the ability of the GB/SA solvation model to provide a quantitative estimate for this barrier should be questioned. An explicit solvent representation would overcome this limitation. Unfortunately its computational cost would be prohibitive for the present case.

Our previous experience with using the same solvation model indicates that this type of calculation correctly reproduces relative mechanical stability of many proteins. In particular, the relative mechanical stabilities of the I27 domain of the muscle protein titin,[17] ubiquitin, and protein G[9] obtained from our simulations are in close agreement with experiments.[11,59] Moreover, the computed relative mechanical stabilities of the same domain with respect to different ways of pulling it[18] are also in close agreement with experimental studies.[10] We believe that the success of the method is partly due to the fact the mechanical stability of a protein is largely determined by its native topology[7,60] (and pulling geometry), which is why even cruder, minimalist, off-lattice models do reasonably good job predicting the mechanical response of proteins.[23,61]

With the above caveats in mind, our main findings discussed below still await their experimental verification. Our calculations suggest that the protein G dimer is less resistant to mechanical pulling than its monomeric counterpart. Nevertheless, it exhibits considerable mechanical stability. Moreover, the mechanical unfolding mechanism for this dimer resembles closely that observed in the I27 domain of the muscle protein titin, ubiquitin, and the protein G monomer. All these proteins share the same structural feature, the presence of terminal parallel strands, which is responsible for their high mechanical resistance with respect to the stretching between their C- and N-termini. The mechanical unfolding pathway then involves the separation of the parallel strands accompanied by the breaking of several hydrogen bonds. As those bonds are loaded in parallel, their concerted rupture requires a high force.

The significant strength of the "clamp" formed by the terminal parallel strands results in the rest of the protein structure being "protected" from the stretching force until the strands become separated. In other words, no domain unfolding (or partial unfolding) occurs prior to the separation of the terminal strands. Interestingly, similar behavior was found in a recent simulation study of the forced dissociation of an adhesion protein complex in the regime where the applied force was ramped slowly enough.[20]

It is not inconceivable that the mechanical response of natural fibers, adhesives, and composites could be optimized both at the single chain level and at the mesoscopic level through interactions among individual chains.

In contrast to the plethora of experimental data on the mechanical response of individual protein domains, single molecule pulling studies of noncovalently bound protein complexes have begun only recently.[12,13] Although recent AFM pulling studies of spider silk[62] and other natural materials[1], in principle, locally probe one or several polypeptide chains that are noncovalently cross-linked with other proteins, the precise system that is being mechanically loaded and the manner in which the loading is done is not well defined (and is likely to vary from pull to pull). Schwaiger et al.[13] have studied the mechanical response of the much better characterized ddFLN dimer. While their study mainly focused on the unfolding of individual domains within each monomer, they point out that the dimer bond is strong enough to stay intact while those domains are unfolding. They further estimate the lower bound on the average dimer separation force to be ∼200 pN at the pulling rate used in the experiments. Unfortunately, direct measurement of the dimer bond strength was precluded by the fact that it is hard to distinguish separation of the two monomers from desorption of the entire molecule from either the AFM tip or the substrate. We hope that computational studies such as this one will provide estimates of the unfolding forces that could be anticipated in such experiments and stimulate future experimental studies.

Acknowledgment. We would like to thank James C. Hu for drawing our attention to dimers and D. Alastair Smith for the comments regarding the experimental feasibility of the proposed measurement. This work was supported by the Robert A. Welch Foundation, the ACS Petroleum Research Fund, and by the National Science Foundation CAREER award to D.E.M. The CPU time was provided by the Texas Advanced Computer Center.

References and Notes

(1) Smith, B. L.; Schaffer, T. E.; Viani, M.; Thompson, J. B.; Frederick, N. A.; Kindt, J.; Belcher, A.; Stucky, G. D.; Morse, D. E.; Hansma, P. K. *Nature* **1999**, *399*, 761.

(2) Lavery, R.; Lebrun, A.; Allemand, J.-F.; Bensimon, D.; Croquette, V. *J. Phys.: Condens. Matter* **2002**, *14*, R383−R414, 2002.

(3) Best, R. B.; Brockwell, D. J.; Toca-Herrera, J. L.; Blake, A. W.; Smith, D. A.; Radford, S. E.; Clarke, J. *Anal. Chim. Acta* **2003**, *479*, 87−105.

(4) Bustamante, C.; Chemla, Y. R.; Forde, N. R.; Izhaky, D. *Annu. Rev. Biochem.* **2004**, *73*, 705−748.

(5) Best, R. B.; Li, B.; Steward, A.; Daggett, V.; Clarke, J. *Biophys. J.* **2001**, *81*, 2344.

(6) Brockwell, D. J.; Paci, E.; Zinober, R. C.; Beddard, G. S.; Olmsted, P. D.; Smith, D. A.; Perham, R. N.; Radford, S. E. *Nat. Struct. Biol.* **2003**, *10*, 731.

(7) Eom, K.; Li, P.-C.; Makarov, D. E.; Rodin, G. J. *J. Phys. Chem. B* **2003**, *107*, 8730.

(8) Eom, K.; Makarov, D. E.; Rodin, G. J. *Phys. Rev. E* **2005**, *71*, 021904.

(9) Li, P.-C.; Makarov, D. E. *J. Phys. Chem. B* **2004**, *108*, 745−749.

(10) Carrion-Vazquez, M.; Li, H.; Lu, H.; Marszalek, P. E.; Oberhauser, A. F.; Fernandez, J. M. *Nat. Struct. Biol.* **2003**, *10*, 738.

(11) Brockwell, D. J.; Beddard, G. S.; Paci, E.; West, D. K.; Olmsted, P. D.; Smith, D. A.; Radford, S. E. *Biophys. J.* **2005**, *89*, 506−519.

(12) Law, R.; Harper, S.; Speicher, D. W.; Discher, D. E. *J. Biol. Chem.* **2004**, *279*, 16410−16416.

(13) Schwaiger, I.; Kardinal, A.; Schleicher, M.; Noegel, A. A.; Rief, M. *Nat. Struct. Mol. Biol.* **2003**, *11*, 81−85.

(14) Lu, H.; Isralewitz, B.; Krammer, A.; Vogel, V.; Schulten, K. *Biophys. J.* **1998**, *75*, 662.

(15) Lu, H.; Schulten, K. *Chem. Phys.* **1999**, *247*, 141.

(16) Isralewitz, B.; Gao, M.; Schulten, K. *Curr. Opin. Struct. Biol.* **2001**, *11*, 224−230.

(17) Li, P.-C.; Makarov, D. E. *J. Chem. Phys.* **2003**, *119*, 9260.

(18) Li, P.-C.; Makarov, D. E. *J. Chem. Phys.* **2004**, *121*, 4826.

(19) Paci, E.; Karplus, M. *J. Mol. Biol.* **1999**, *288*, 441−459.

(20) Bayas, M. V.; Schulten, K.; Leckband, D. *Biophys. J.* **2003**, *84*, 2223−2233.

(21) Bayas, M. V.; Schulten, K.; Leckband, D. *Mech. Chem. Biosyst.* **2004**, *1*, 101−111.

(22) Liu, Y.; Gotte, G.; Libonati, M.; Eisenberg, D. *Nat. Struct. Biol.* **2001**, *8*, 211−214.

(23) Kirmizialtin, S.; Huang, L.; Makarov, D. E. *J. Chem. Phys.* **2005**, *122*, 234915.

(24) Brockwell, D. J.; Beddard, G. S.; Clarkson, J.; Zinober, R. C.; Blake, A.; Trinick, J.; Olmsted, P. D.; Smith, D. A.; Radford, S. E. *Biophys. J.* **2002**, *83*, 458.

(25) Carrion-Vazquez, M.; Oberhauser, A. F.; Fowler, S. B.; Marsalek, P. E.; Broedel, S. E.; Clarke, J.; Fernandez, J. M. *Proc. Natl. Acad. Sci. U.S.A.* **1999**, *96*, 3694−3699.

(26) Schwaiger, I.; Sattler, C.; Hostetter, D. R.; Rief, M. *Nat. Mater.* **2002**, *1*, 232.

(27) Lacks, D. J. *Biophys. J.* **2005**, *88*, 3494−3501.

(28) Matouschek, A. *Curr. Opin. Struct. Biol.* **2003**, *13*, 98−109.

(29) Matouschek, A.; Bustamante, C. *Nat Struct Biol* **2003**, *10*, 674−676.

(30) Prakash, S.; Matouschek, A. *TIBS* **2004**, *29*, 593−600.

(31) Liu, Y.; Eisenberg, D. *Prot. Sci.* **2002**, *11*, 1285.

(32) Frank, M. K.; Dyda, F.; Dobrodumov, A.; Gronenborn, A. M. *Nat. Struct. Biol.* **2002**, *9*, 877−885.

(33) Byeon, I.-J. L.; Louis, J. M.; Gronenborn, A. M. *J. Mol. Biol.* **2003**, *333*, 141−152.

(34) Gronenborn, A. M.; Filpula, D. R.; Essig, N. Z.; Achari, A.; Whitlow, M.; Wingfield, P. T.; Clore, G. M. *Science* **1991**, *253*, 657−61.

(35) McCammon, J. A.; Harvey, S. C. *Dynamics of proteins and nucleic acids*; Canbridge University Press: Cambridge, 1987.

(36) Frenkel, D.; Smit, B. *Understanding Molecular Simulation*, 2nd ed.; Academic Press: San Diego, San Francisco, New York, Boston, London, Sydney, Tokyo, 2002.

(37) Sugita, Y.; Okamoto, Y. *Chem. Phys. Lett.* **1999**, *314*, 141−151.

(38) Qiu, D.; Shenkin, P. S.; Hollinger, F. P.; Still, W. C. *J. Phys. Chem. A* **1997**, *101*, 3005.

(39) Wang, J.; Cieplak, P.; Kollman, P. A. *J. Comput. Chem.* **2000**, *21*, 1049−1074.

(40) Andersen, H. C. *J. Comput. Phys.* **1983**, *52*, 24−34.

(41) Rief, M.; Fernandez, J. M.; Gaub, H. E. *Phys. Rev. Lett.* **1998**, *81*, 4764.

(42) Bell, G. I. *Science* **1978**, *200*, 618−627.

(43) Evans, E.; Ritchie, K. *Biophys. J.* **1997**, *72*, 1541−1555.

(44) Evans, E.; Ritchie, K. *Biophys. J.* **1999**, *76*, 2439.

(45) Marsalek, P. E.; Lu, H.; Li, H.; Carrion-Vazquez, M.; Oberhauser, A. F.; Schulten, K.; Fernandez, J. *Nature* **1999**, *402*, 100.

(46) Rief, M.; Gautel, M.; Oesterhelt, F.; Fernandez, J. M.; Gaub, H. E. *Science* **1997**, *276*, 1109−1112.

(47) Oberhauser, A. F.; Hansma, P. K.; Carrion-Vazquez, M.; Fernandez, J. M. *Proc. Natl. Acad. Sci U.S.A.* **2001**, *98*, 468−472.

(48) Fernandez, J. M.; Li, H. *Science* **2004**, *303*, 1674−8.

(49) Schlierf, M.; Li, H.; Fernandez, J. M. *Proc. Natl. Acad. Sci U.S.A.* **2004**, *101*, 7299.

(50) Zhou, R. *Proteins* **2003**, *53*, 148−161 2003.

(51) Ben-Naim, A.; *J. Chem. Phys.* **1990**, *93*, 8196.

(52) Ben-Naim, A.; *J. Phys. Chem.* **1990**, *94*, 6893−6895.

(53) Bruge, F.; Fornili, S. L.; Malenkov, G. G.; Palma-Vittorelli, M. B.; Palma, M. U. *Chem. Phys. Lett* **1996**, *254*, 283−291.

(54) Durell, S. R.; Brooks, B. R.; Ben-Naim, A. *J. Phys. Chem.* **1994**, *98*, 2198−2202.

(55) Hassan, S. A. *J. Phys. Chem. B* **2005**, *109*, 21989.

(56) Li, X.; Hassan, S. A.; Mehler, E. L. *Proteins* **2005**, *60*, 464.

(57) Hassan, S. A.; *J. Phys. Chem. B* **2004**, *108*, 19501−19509.

(58) Hassan, S. A.; Guarnieri, F.; Mehler, E. L. *J. Phys. Chem. B* **2000**, *104*, 6478−6489.

(59) Cao, Y.; Lam, C.; Wang, M.; Li, H. *Angew. Chem., Int. Ed. Engl.* **2006**, *45*, 642−645.

(60) Klimov, D. K.; Thirumalai, D. *Proc. Natl. Acad. Sci. U.S.A.* **2000**, *97*, 7254.

(61) West, D. K.; Brockwell, D. J.; Olmsted, P. D.; Radford, S. E.; Paci, E. *Biophys. J.* **2006**, *90*, 287−297.

(62) Becker, N.; Oroudjev, E.; Mutz, S.; Cleveland, J. P.; Hansma, P. K.; Hayashi, C. Y.; Makarov, D. E.; Hansma, H. G. *Nat. Mater.* **2003**, *2*, 278.

(63) Koradi, R.; Billeter, M.; Wüthrich, K. *J. Mol. Graph.* **1996**, *14*, 51−55.